Supporting Information

Bartumeus and Levin 10.1073/pnas.0801926105

SI Text

Sampling of Probability Distributions. By applying the inversion method (1) on the wrapped Cauchy distribution (WCD) we obtain that the angle deviations θ from a preferred direction ϕ follows:

$$\theta = \phi + 2\arctan\left[\left(\frac{1-\rho}{1+\rho}\right)\tan\left[\pi\left(u - \frac{1}{2}\right)\right]\right],$$

where u is a uniformly distributed random variable in the interval $u \in [0,1]$, and ρ is the shape parameter of the probability distribution $\rho \in [0,1]$. We set $\phi = 0$ so the WCD accounts for the tendency, observed in many organisms, to maintain the previous directions while scanning, whereas the shape parameter ρ of the WCD, controls the sinuosity and the correlation length of the walk (2, 3). Tuning the shape parameter ρ one can go from Brownian ($\rho = 0$) to ballistic movement ($\rho = 1$) (i.e., straight-line searching) (4).

In the LMCRW model we generate the successive reorientation time intervals by sampling the power law distribution in the following way (inversion method; ref. 1) $t = t_0 u^{(1-\mu)^{-1}}$, where t_0 is the minimum time step ($t_0 = 1$) and u is a random uniformly distributed variable within the interval $u \in [0,1]$.

For the non-Lévy intermittent model we sample an exponential distribution with characteristic time τ (inversion method; ref. 1) $t = \ln(ue^{-t_0/\tau})\tau$, where t_0 is the minimum time step ($t_0 = 1$) and u is a random uniformly distributed variable within the interval $u \in [0,1]$. We define the characteristic time as $\tau = \beta\lambda_p$, where $\beta \in [0.01,1]$ and λ_p is the average distance between patches (see section above). Thus, the range of τ chosen represents from 1% to 100% of the average travel time between patches. The latter is proportional to λ_p under the assumption that the searchers move mostly in straight lines and with constant velocity.

Scaling of Simulations and Target Landscapes. The mean free path (i.e., λ) is defined as the average Euclidean distance between target sites, hence, it has 1D spatial units. To make comparable the encounter rates of diffusive-like searching processes at distinct dimensional space (i.e., 2D, 3D) we need to fix the mean free path (i.e., λ) at a constant value so that the searchers have similar probabilities to find the targets (4, 5). To compute λ we need to know the characteristic one-dimensional length (1D) of the searching arena L, the number of target sites N, and the detection distance R, i.e., the sum of the "radius of vision" of the searcher and the target ($R = r_t + r_s$). The mean free path is given by $\lambda = L^2/2RN$ (2D) and $\lambda = L^3/\pi R^2 N$ (3D) (4, 5). From the equations above one can see that λ is inversely related to the target density, i.e., $\lambda \sim 1/\nu$, where $\nu_{2\mathrm{D}} = NL^{-2}$ and $\nu_{3\mathrm{D}} = NL^{-3}$.

By fixing the number of targets $N_t = 50$ and the detection distance $R = 1$ we compute two average distances between patches representing two different resource densities: $\lambda_p = 100$ (i.e., high-resource scenario) and $\lambda_p = 1{,}000$ (i.e., low-resource scenario). Within each dimensional system then, λ_p represents a resource density. However, when we compare different dimensional systems such as $\lambda_{p\text{-2D}} = \lambda_{p\text{-3D}} = 100$, one must note that to keep the same λ_p in different dimensionalities, the characteristic length of the searching arena L must change if the number of target sites N is fixed. Hence, although $\lambda_{p\text{-2D}}$ and $\lambda_{p\text{-3D}}$ are equal, therefore the average probability of finding a target in the landscape is maintained, the target densities i.e., $\nu_{2\mathrm{D}}$ and $\nu_{3\mathrm{D}}$ are different.

To generate the patchy landscapes, we first locate five source points in a uniformly distributed arrangement covering the whole landscape. Each of these five points acts as a "seed" for building up the patches. Each patch consists of 10 target sites randomly located with an exponentially decaying radial distribution centered at the seed position. This procedure leads to a uniform distribution of patches, all of them having the same number of Poisson-distributed targets. The "local" density in each patch is defined by the characteristic spatial scale of the exponential distribution, $\sigma = 0.025L$. Thus, the local density changes according to the size of L, whereas the "global" density can be set independently of L. Each detected and consumed target is replaced in the arena considering the original source-patch from where it came from.

By construction, both the average distance between patches λ_p and the average distance between targets λ_t (more related to the global density) can be calculated in our landscapes. In high-resource scenarios we have $\lambda_p = 100$ that corresponds to $\lambda_t = 10$. In low-resource scenarios we have $\lambda_p = 1{,}000$ that corresponds to $\lambda_t = 100$. Nevertheless, in patchy landscapes, the average distance between patches λ_p is much more representative of the average global density of targets than the average distance between targets λ_t, being λ_p the most informative landscape parameter. The scaling parameter λ_p that we choose in our patchy landscapes (i.e., $\lambda_p = 100$ and $\lambda_p = 1{,}000$) could represent, for example in a 3D system, patchy prey distributions with density ranges representing two main marine resource scenarios: coastal productive areas (i.e., from 10^3 to 10^4 cell per ml) and open ocean areas (i.e., from 10^1 to 5×10^2 cell per ml), respectively.

In the fractal-like landscapes, target locations represent the points visited by a Lévy flight, the so-called Lévy dust (6), with Lévy index $\mu = 2$. We maintained the same scaling conditions as for the patchy landscapes by fixing the number of targets N and the detection distance $R = 1$. Note, however, that for these types of landscapes the average distance between patches λ_p is not really informative. In these landscapes, detected and consumed targets are replaced by new flights that have its origin in the last placed target. Although encounters destroy the Lévy dust structure, fractal-like properties are maintained in the landscape through the replacement of new targets that contribute to generate new Lévy dust, thus balancing the loss of structure caused by targets' disappearances. Of note is the fact that such a process might not easily reach a statistical equilibrium, hence, the results obtained for fractal-like landscapes can be comparable between them but might not be straightforwardly comparable to the ones obtained in the patchy-landscape simulations, where a statistical equilibrium and nontransient behaviors can be assumed.

In all simulations, we set a searcher fixed-step length and a velocity equal to the radius of vision $\ell_0 = \nu_s = r_s = r_\mathrm{t} = 0.5$, and we compute the average and the standard deviation of the search efficiency (i.e., η) over 10 random walkers that travel a total of $N = 10^7$ steps in 10 Monte Carlo replications of each type of landscape: patchy and fractal-like.

Pointwise Model Selection (PWMS) Tests. The PWMS consist of conducting sequential maximum likelihood fits and model selection tests on subsets of a sample data (N). Model selection is based on Akaike Information Criteria (AIC) weights, corrected for small data samples (wAICc) (7, 8), which determine the likelihood of a subset being fitted better by one model than the other. The data are arranged in ascending order. Starting from the smallest value, at each iteration (i), we obtain a subset of size ($N - i$). Each time (i), two probabilistic models, an exponential distribution (the simplest decaying function) and a uniform distribution (UD), are confronted to fit by maximum likelihood the resulting subset of the sampled data. The weight of evidence that each subset N-i fits better one model than the other is then computed through the AIC weights. For each iteration (i) the AIC weights (i.e. wAICc) are then plotted as a function of the size ($N - i$) of each fitted subset. To show the average behavior of the PWMS tests for our null model, the nonintermittent model, we generate 100 Monte-Carlo series of turning angles (of length N) gleaned from a WCD ($\rho = 0.9$). If the results of the PWMS tests at the tail of the two turning-angle distributions (obtained with the nonintermittent and the intermittent model, respectively) fall within the range of the observed results for the Monte Carlo series, we can assume that the tail of the turning angle distribution is not statistically different from the expected tail in the null (nonintermittent) model, hence, we should assume absence of intermittence in the trajectory. If intermittence exists, the PWMS procedure can tell us the exact regime of turning angle values for which we can expect to "observe" such phenomena. It also can show us the critical turning angle θ_c where the transition in weight of evidence (wAICc) from an exponential to a uniform distribution has occurred. Taking the critical turning angle θ_c (or otherwise its double, to ensure that we are not at the transition regime) and computing the time intervals between turning angles θ such as $\theta \geq \theta_c$, we can recover the scaling exponent μ that characterizes the Lévy-intermittent behavior.

Lévy Intermittence Compared with Enhanced Perceptual Capabilities and Speed. We compare the effects on search efficiency of Lévy-intermittent searching with nonintermittent searches (only scanning behavior exists) where the searcher perceptual capabilities (or equivalently size) and speed are gradually increased. Fig. S2*a* shows that with a 2D nonintermitent search, velocity should increase almost by 2-fold and the perceptual range (or size) by 4-fold to obtain similar search efficiencies (up to a 50% of search gain) as for an optimal Lévy-intermittent search (dashed line in Fig. S2*a*). In 3D systems (Fig. S2*b*), the net effect of optimal Lévy intermittence (dashed line in Fig. S2*b*) is decreased, but still can represent an efficiency gain equivalent in the nonintermittent model to an increase of 1.5-fold in speed or size. Interestingly, in 3D systems, perceptual capability (or size) is more important than speed to increase encounter rates, whereas in 2D systems encounter rates are more sensitive to speed than to perceptual capabilities.

Considering the energetic costs associated with enhancing search efficiency by increasing the cruising speed and/or the perceptual capabilities the timing of specific reorientation mechanisms search surely must be a strong target for natural selection. The reorientation mechanisms providing an optimal Lévy intermittence could be strongly favored, but more generally, natural selection could favor mechanisms controlling a whole range of Lévy indexes, which would allow animals for efficient adjustments of average contact rates on the basis of some "reorientation plan of action" triggered by coarse-grained, landscape level environmental cues (e.g., absence/presence of mates, absence/presence of predators, absence/presence of resource).

1. Press WH, Teukolsky SA, Vetterling WT, Flannery BP (1992) *Numerical Recipes in C: The Art of Scientific Computing* (Cambridge Univ Press, Cambridge, UK).
2. Viswanathan G, Raposo E, Bartumeus F, Catalan J, da Luz MGE (2005) Necessary criterion for distinguishing true superdiffusion from correlated random walk processes. *Phys Rev E* 72:1–6.
3. Bartumeus F, Catalan J, Viswanathan GM, Raposo EP, da Luz MGE (2008) The influence of turning angles on the success of nonorientated animal searches. *J Theor Biol* 252:43–55.
4. Bartumeus F, Da Luz MGE, Viswanathan GM, Catalan J (2005) Animal search strategies: A quantitative random-walk analysis. *Ecology* 86:3078–3087.
5. Bartumeus F, *et al.* (2008) Superdiffusion and encounter rates in diluted, low dimensional worlds. *Eur Phys J Special Topics* 157:157–166.
6. Mandelbrot BB (1977) *Fractals: Form, Chance, and Dimension* (Freeman, San Francisco).
7. Hilborn R, Mangel M (1997) *The Ecological Detective: Confronting Models with Data* (Princeton Univ Press, Princeton).
8. Burnham KP, Anderson DR (2002) *Model Selection and Inference. A Practical Information-Theoretical Approach* (Springer, Berlin), 2nd Ed.

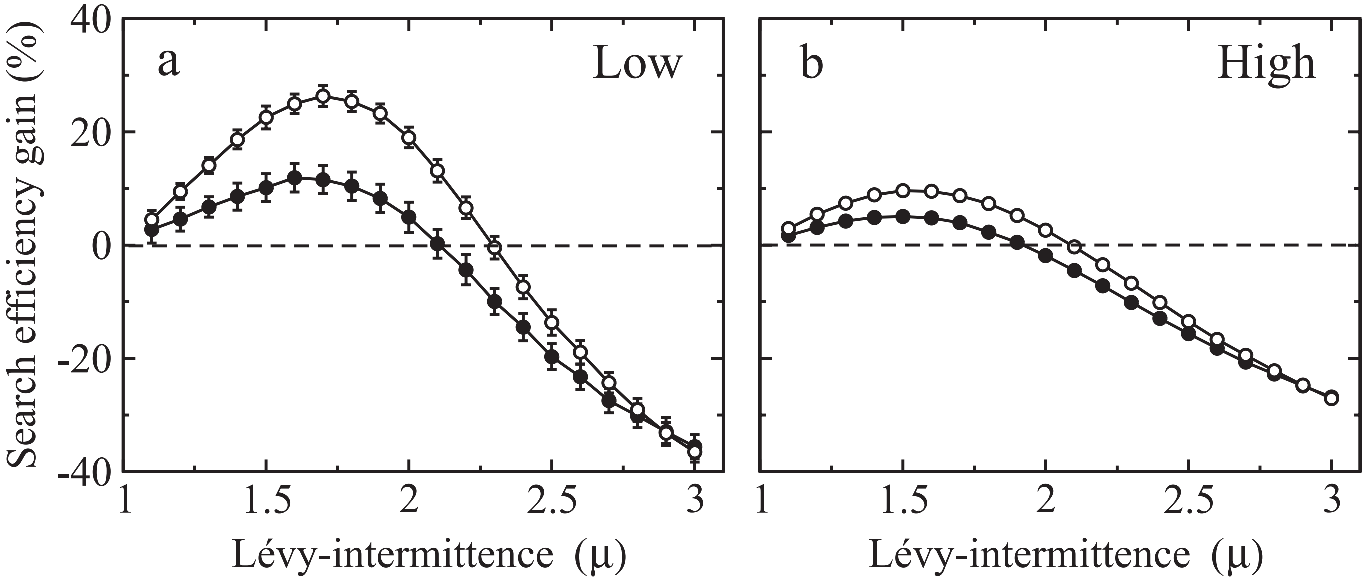

Fig. S1. Search efficiency gain $\Delta\eta(\%)$ comparing search processes with and without Lévy intermittence in 2D fractal-like landscapes. Results are shown for low, i.e., $\lambda_p = 1{,}000$ (*a*), and high, i.e., $\lambda_p = 100$ (*b*) patch densities, for different scanning behaviors: $\rho = 0.7$ (●) and $\rho = 0.9$ (○), and for different Lévy-intermittent reorientation behaviors ($1 < \mu \leq 3$). Dashed lines indicate, zero search efficiency gain ($\Delta\eta = 0\%$).

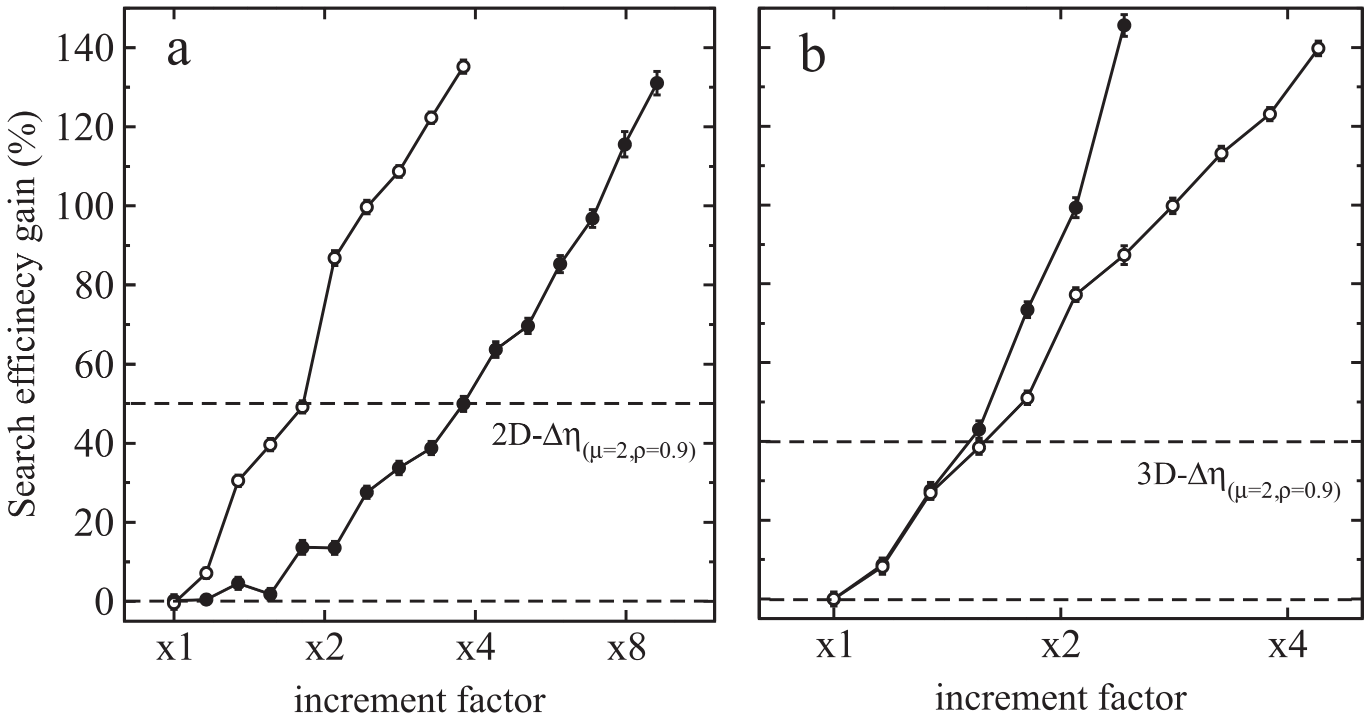

Fig. S2. Search efficiency gain $\Delta\eta$ (%) in the absence of Lévy intermittence caused by an increase in size (●) and velocity (○). Results are shown for 2D (*a*) and 3D (*b*) patchy landscapes. In all cases, scanning behavior of searchers was set at $\rho = 0.9$, and the initial size and cruising velocity were set at $r = v = 0.5$. Note the logarithmic scale of the *x* axis indicating the increment factors of size and velocity. Dashed lines indicate the maximum range of change in search efficiency observed for optimal Lévy-intermittent searches $\Delta\eta(\mu \sim 2,\ \rho = 0.9)$ (see Fig. 1).